ARTICLE
Journal of Cellular Biochemistry 112:881–893 (2011)

Journal of Cellular Biochemistry

# ACSL3 and GSK-3β Are Essential for Lipid Upregulation Induced by Endoplasmic Reticulum Stress in Liver Cells

Yung-Sheng Chang,[1,2] Chien-Ting Tsai,[1] Chien-An Huangfu,[1] Wen-Ya Huang,[3,4] Huan-Yao Lei,[5] Chiou-Feng Lin,[6] Ih-Jen Su,[7] Wen-Tsan Chang,[1] Pei-Huan Wu,[1] Ya-Ting Chen,[3] Jui-Hsiang Hung,[8] Kung-Chia Young,[3*] and Ming-Derg Lai[1,2,4*]

[1]*Department of Biochemistry and Molecular Biology, College of Medicine, National Cheng Kung University, Tainan, Taiwan*

[2]*Institute of Basic Medical Sciences, College of Medicine, National Cheng Kung University, Tainan, Taiwan*

[3]*Department of Medical Laboratory Science, College of Medicine, National Cheng Kung University, Tainan, Taiwan*

[4]*Center for Gene Regulation and Signal Transduction Research, College of Medicine, National Cheng Kung University, Tainan, Taiwan*

[5]*Department of Microbiology and Immunology, College of Medicine, National Cheng Kung University, Tainan, Taiwan*

[6]*Institute of Clinical Medical Sciences, College of Medicine, National Cheng Kung University, Tainan, Taiwan*

[7]*Division of Clinical Research, National Health Research Institute, Tainan, Taiwan*

[8]*Department of Biotechnology, Chia Nan University of Pharmacy and Science, Tainan, Taiwan*

## ABSTRACT

The endoplasmic reticulum (ER) is essential for lipid biosynthesis, and stress signals in this organelle are thought to alter lipid metabolism. Elucidating the mechanisms that underlie the dysregulation of lipid metabolism in hepatocytes may lead to novel therapeutic approaches for the treatment of lipid accumulation. We first tested the effects of several inhibitors on lipid dysregulation induced by tunicamycin, an ER stress inducer. Triacsin C, an inhibitor of long-chain acyl-CoA synthetase (ACSL) 1, 3, and 4, was the most potent among these inhibitors. We then analyzed the expression of the ACSL family during ER stress. The expression of ACSL3 was induced by ER stress in HuH-7 cells and in mice livers. ACSL3 shRNA, but not ACSL1 shRNA, inhibited the induction of lipid accumulation. GSK-3β inhibitors attenuated ACSL3 expression and the lipid accumulation induced by ER stress in HuH-7 cells. shRNA that target GSK-3β also inhibited the upregulation of ACSL3 and lipid accumulation in HuH-7 and HepG2 cells. The hepatitis B virus mutant large surface protein, which is known to induce ER stress, increased the lipid content of cells. Similarly, Triacsin C, and GSK-3β inhibitors abrogated the lipid dysregulation caused by the hepatitis B virus mutant large surface protein. Altogether, ACSL3 and GSK-3β represent novel therapeutic targets for lipid dysregulation by ER stress. J. Cell. Biochem. 112: 881–893, 2011. 

**KEY WORDS:** ACSL3; GSK-3BETA; LIPID DYSREGULATION; ENDOPLASMIC RETICULUM STRESS

The liver is an essential organ for the maintenance of homeostasis of lipid metabolism in the human body. The dysregulation of lipid metabolism has been associated with many diseases, including type II diabetes mellitus, fatty liver syndrome, and hepatocarcinoma [Reddy and Rao, 2006; Hsu et al., 2007; Starley et al., 2010]. Lipid metabolism has also been linked to numerous cellular processes [Wang et al., 2006; Gaspar et al., 2008]. The formation of lipid droplets is considered not only as a system to store energy but also is thought to be involved in many physiological processes [Goodman, 2008; Thiele and Spandl, 2008]. Fatty acids are synthesized by an extramitochondrial system that involves the cytosol and the endoplasmic reticulum (ER). The first

Additional Supporting Information may be found in the online version of this article.

Grant sponsor: National Science Council; Grant number: NSC 95-2311-B-006-001; Grant sponsor: National Cheng Kung University; Grant number: B035; Grant sponsor: Comprehensive Cancer Center in Southern Taiwan; Grant number: DOH99-TD-C-111-03.

*Correspondence to: Dr. K.-C. Young or Prof. M.-D. Lai, No.1 University Road, Tainan 701, Taiwan.
E-mail: t7908077@mail.ncku.edu.tw, a1211207@mail.ncku.edu.tw

Received 16 June 2010; Accepted 2 December 2010 • DOI 10.1002/jcb.22996 • © 2010 Wiley-Liss, Inc.
Published online 29 December 2010 in Wiley Online Library (wileyonlinelibrary.com).

step in fatty acid synthesis is the conversion of acetyl CoA to malonyl-CoA by acetyl-CoA carboxylase. Malonyl-CoA is then used as the building block for long-chain fatty acid synthesis by fatty acid synthase in the cytosol. The fatty acid elongase in the endoplasmic reticulum elongates saturated or unsaturated fatty acyl-CoA (from C10 upward) by two carbons and uses malonyl-CoA as a carbon donor. The fatty acids are eventually incorporated into triacylglycerol or other complex lipids. The first enzyme that regulates the synthesis of triacylglycerol is acyl-CoA synthetase [Coleman et al., 2000]. The acyl-CoA synthetases can be subdivided into five subfamilies based on the lengths of their fatty acid substrates: short-chain acyl-CoA synthetases, medium-chain acyl-CoA synthetases, long-chain acyl-CoA synthetases, bubblegum acyl-CoA synthetases, and very long-chain acyl-CoA synthetases. Long-chain acyl-CoA synthetases (ACSLs) catalyze the first step in fatty acid metabolism by converting long-chain fatty acid into acyl-CoA thioesters and enter both anabolic and catabolic pathways. There are five family members of mammalian ACSLs: ACSL1, 3, 4, 5, and 6. ACSL family members have different cellular localization patterns. ACSL1 is associated with the plasma membrane and also found in lipid droplets, microsome, and mitochondria. ACSL3 is presented in lipid droplets and ER membrane. ACSL4 can be detected in peroxisome and ER. ACSL5 is expressed in mitochondria, ER, and plasma membrane. ACSL6 is mainly presented in plasma membrane [Lewin et al., 2001; Soupene and Kuypers, 2008; Obata et al., 2010]. The physiological functions of ACSLs have been recently investigated. For example, ACSL6 gene was found to be associated with premature ovarian failure [Kang et al., 2009]. In addition, Triacsin C, a selective inhibitor of acyl-CoA synthetase, reduced atherosclerotic areas in the aorta and hearts in low-density lipoprotein receptor-knockout mice [Matsuda et al., 2008].

The ER is an important organelle for lipid metabolism and membrane/secretory protein biosynthesis. Many exogenous agents and the overexpression of endogenous proteins can produce ER stress, which subsequently initiates signaling cascades that are associated with pathological alterations. For example, during chronic hepatitis B virus infection, the expression of mutant hepatitis B large surface proteins lead to endoplasmic reticulum stress, which have been linked to hepatocarcinogenesis [Hung et al., 2004; Wang et al., 2005; Yang et al., 2009]. These ER stress signal transduction pathways can be studied with drugs that perturb ER function, including the glycosylation inhibitor tunicamycin. Unfolded proteins in the endoplasmic reticulum activate several signaling pathways that are referred to as the unfolded protein responses (UPR). In mammalian cells, the proximal responder IRE1α/β activates the unconventional splicing of the XBP1 mRNA. The spliced XBP-1 mRNA is translated into an active XBP-1 protein. Inactive ATF6 is also cleaved to produce the active ATF6 form during ER stress [Ye et al., 2000]. Activated XBP-1 and ATF6 induce a set of chaperones that aid protein folding. Several chaperones have been shown to be required for ER protein folding, such as Bip/GRP78, GRP94, and protein disulfide isomerase. Translational inhibition is mediated by the ER kinase PERK, which is activated during UPR. PERK phosphorylates the general translation factor eIF2α and downregulates translation. In addition, PERK activates the translation of ATF4 [Harding et al., 2000]. In addition to ATF4 and ATF6, UPR triggers activation of the transcription factor NF-κB [Pahl and Baeuerle, 1996]. NF-κB activation has been suggested to require the release of calcium from the ER and the production of reactive oxygen species [Pahl and Baeuerle, 1996]. Phosphorylation of the alpha subunit of eukaryotic initiation factor 2 by PERK is required for the activation of NF-κB in response to endoplasmic reticulum stress [Jiang et al., 2003]. IRE1 is also involved in the activation of NF-κB [Hu et al., 2006]. We have characterized the NF-κB response and found that NF-κB was activated through multiple pathways, including calcium signaling and pp38 kinase [Hung et al., 2004]. In addition to the ERK signal pathways, UPR has been shown to regulate glycogen synthase kinase (GSK) 3β which is essential for the regulation of p53 and cyclin D1 degradation during early ER stress [Pluquet et al., 2005; Raven et al., 2008]. In addition to p53, GSK-3β regulates the activation of caspase 2 during ER stress in leukemia [Huang et al., 2009].

Because the ER is an important organelle for lipid biosynthesis, endoplasmic reticulum stress has been hypothesized to alter lipid metabolism. XBP-1, ATF6, eIF2α, and IRE1 have been demonstrated to play an important role in the dysregulation of lipid metabolism in hepatocytes [Gaspar et al., 2008; Lee et al., 2008; Oyadomari et al., 2008; Rutkowski et al., 2008]. However, the connection between ER stress and the dysregulation of lipid metabolism is not completely understood. Because this dysregulation has been linked to many diseases, it is important to investigate how lipid upregulation is attenuated by ER stress in the liver. In this report, we screened several inhibitors and identified an ACSL family gene as one of the essential mediators. Our results demonstrate that ACSL3 is essential for lipid accumulation. Furthermore, GSK-3β is an upstream regulator of the ACSL family and of lipid accumulation in hepatocytes.

## EXPERIMENTAL PROCEDURES

### CHEMICALS AND KITS

Tunicamycin, brefeldin A, thapsigargin, ethidium bromide, SDS, Bay 11-7082, Oil red O, G418 sulfate, cycloheximide, 2-amino-purine, lithium chloride, and Triacsin C were purchased from Sigma (St. Louis, MO). PD98059, JNK inhibitor II, GSK-3β inhibitor VIII, and the secondary rabbit anti-goat horseradish peroxidase-conjugated antibody were purchased from Calbiochem (La Jolla, CA). The ECL Western blot detection system was purchased from Millipore (Bedford, MA). The RT-PCR reagents were purchased from Promega (Madison, WI). The Micro BCA™ protein assay reagent kit was purchased from Pierce (Woburn, MA), and the anti-GRP78 antibody was purchased from Transduction Laboratories (Lexington, KY). The anti-ACSL1, anti-phospho-GSK-3β (Ser9), secondary horse anti-mouse horseradish peroxidase-conjugated, and secondary horse anti-rabbit horseradish peroxidase-conjugated antibodies were purchased from Cell Signaling (Beverly, MA). The anti-GSK-3α/β, ACSL3, and ACSL5 antibodies were purchased from Santa Cruz Biotechnology (Santa Cruz, CA). The anti-ACSL4 and ACSL6 antibodies were purchased from Abnova (Taiwan). The anti-β-actin and secondary goat anti-rat horseradish peroxidase-conjugated antibodies were purchased from Chemicon (Pittsburgh, PA). The anti-HA antibody was purchased from Roche (Indianapolis, IN).

LipofectAMINE 2000, TRIzol reagent, Dulbecco's modified Eagle's medium (DMEM), and antibiotic mixture (10,000 U of penicillin and 10,000 mg streptomycin) were purchased from Invitrogen (Carlsbad, CA). ProTaq DNA polymerase and REzol C&T were purchased from PROtech Technology, Inc. (Taipei, Taiwan). Oligo(dT) primers were purchased from MDBio (Taiwan). Fetal bovine serum was purchased from Biological Industries (Beit Haemek, Israel), and the Omni TH-115 tissue homogenizer was purchased from Omni Instruments (Warrenton, VA).

### CELL CULTURE AND TREATMENTS

The human hepatocarcinoma HuH-7 cells (JCRB0403) were obtained from JCRB and hepatoblastoma HepG2 cells (ATCC HB-8065) were obtained from ATCC. The mouse ML-1 hepatocarcinoma cell line was obtained from Dr. Huan-Yao Lei. The HuH-7, HuH-7 ACSL1 RNAi transfectants, HuH-7 ACSL3 RNAi transfectants, HepG2, and ML-1 cell lines were maintained at 37°C in a 5% $CO_2$ atmosphere in DMEM supplemented with 10% heat-inactivated fetal bovine serum, 2 mM L-glutamine, 100 U/ml penicillin, and 100 μg/ml streptomycin. HuH-7 cells that express the Pre-S2 deletion of the hepatitis B virus large surface protein were previously established [Hung et al., 2004].

### WESTERN BLOT ANALYSIS

Cell lysates were prepared by treating cells with RIPA lysis buffer (0.22 M NaCl, 0.38 M Tris–HCl, pH 7.5, 0.25% Sodium deoxycholate, and 1% IGEPAL-630). The protein concentration of the supernatant was measured using the Micro BCA™ protein assay reagent kit (Pierce). Approximately 15–25 μg of cell lysates was separated by SDS–PAGE using 10% acrylamide gels and transferred onto polyvinylidene fluoride membranes (Pierce). After blocking with 5% nonfat dry milk for 1 h at room temperature and washing with Tween-20 (TTBS; 25 mM Tris base, 0.02% KCl, 0.8% NaCl, and 0.1% [v/v] Tween-20), the polyvinylidene fluoride membranes were incubated overnight at 4°C with primary antibody in TTBS containing 1% bovine serum albumin. The secondary antibody was subsequently incubated with the membranes for 1 h at room temperature, and the membranes were washed extensively for 40 min with TTBS at room temperature. The catalog number and dilution of antibodies were as the following: the anti-ACSL1 antibody (#4047, 1:1,000 dilution), the anti-ACSL3 antibody (SC-47991, 1:1,000 dilution), the anti-ACSL4 antibody (PAB2504, 1:2,000 dilution), the anti-ACSL5 antibody (SC-47999, 1:2,000 dilution), the anti-ACSL6 antibody (PAB2506, 1:2,000 dilution), the anti-GRP78 antibody (610978, 1:5,000 dilution), the anti-β-actin antibody (MAB1501R, 1:5,000 dilution), the anti-phospho-GSK-3β (Ser9) antibody (#9336, 1:2,000 dilution), the anti-GSK-3α/β antibody (SC-7291, 1:1,000 dilution), the anti-HA antibody (11867423001, 1:4,000 dilution), the secondary horse anti-mouse horseradish peroxidase-conjugated antibody (#7076, 1:2,000 dilution), the secondary goat anti-rabbit horseradish peroxidase-conjugated antibody (#7074, 1:2,000 dilution), the secondary rabbit anti-goat horseradish peroxidase-conjugated antibody (401515, 1:2,000 dilution), and the secondary goat anti-rat horseradish peroxidase-conjugated antibody (AP136P, 1:2,000 dilution). The blots were probed with the ECL Western blot detection system and visualized with the BioSpectrum AC imaging system (UVP, CA) according to the manufacturer's instructions.

### RT-PCR

The cells were washed with cold phosphate-buffered saline (PBS; 137 mM NaCl, 2.7 mM KCl, 10 mM $Na_2HPO_4$, and 1.8 mM $KH_2PO_4$) and lysed with the TRIzol Reagent by repetitive pipetting. Total RNA was extracted according to the manufacturer's instructions (Invitrogen). The mice were sacrificed and their livers were removed. The tissues were homogenized on ice with REzol C&T (PROtech Technology, Inc.) for a few seconds using an Omni TH-115 tissue homogenizer (Omni Instruments). After centrifugation, the supernatant was transferred to an Eppendorf tube, and the total RNA was extracted according to the manufacturer's instructions (PROtech Technology, Inc.). The cDNA was reverse transcribed from 2 μg of total RNA using 5 μM oligo(dT) primers (MDBio) as the template primer and incubated for 5 min at 72°C to melt the RNA secondary structure. After the tubes were cooled on ice, 200 U of Moloney murine leukemia virus (M-MLV) reverse transcriptase (Promega), 0.125 mM dNTP (MDBio), and M-MLV 5× Reaction Buffer (Promega) were added. The reverse transcription was performed 60 min at 42°C for extension and 10 min at 70°C for enzyme inactivation. The 5′ and 3′ human ACSL1 gene-specific primers were 5′-CCA GAA GGG CTT CAA GAC TG -3′ (sense) and 5′-TTT GGG GTT GCC TGT AGT TC-3′ (antisense); the 5′ and 3′ human ACSL3 gene-specific primers were 5′-TGT GCG ACA GCT TTG TTT C-3′ (sense) and 5′-TCC ATC GGG TTC AAA CTC TC-3′ (antisense); the 5′ and 3′ human ACSL5 gene-specific primers were 5′-TCT GAA GCC ACC CTG CTC T-3′ (sense) and 5′-ACA GCG AGT CCT CTT GGG AA-3′ (antisense). The cycling parameters were as follows: 1 min at 94°C for denaturation, 1 min at 52°C for primer annealing, and 1 min at 72°C for extension. Meanwhile, the same amount of cDNA was amplified for 25 cycles using the glyceraldehyde-3-phosphate dehydrogenase gene-specific primers: 5′-TGA AGG TCG GTG TGA ACG GAT TTG GC-3′ (sense) and 5′-CAT GTA GGC CAT GAG GTC CAC CAC-3′ (antisense); GRP78 gene-specific primers: 5′-CGC CTC ATC GGA CGC ACT TG-3′ (sense) and 5′-AGG TTC CAC CGC CCA GGT CA-3′ (antisense). The cDNA was amplified by ProTaq DNA polymerase (PROtech Technology, Inc.). The products were visualized after electrophoresis on a 1.5% agarose gel containing ethidium bromide (0.16 mg/ml final concentration). The signal intensity of the bands was quantified with the Image J densitometry software (National Institutes of Health, Bethesda, MD, USA).

### QUANTITATIVE REVERSE TRANSCRIPTION-PCR

cDNA was prepared as described previously. Quantitative PCR was performed on an ABI 7900 Fast Real-Time system (Applied Biosystems, Foster City, CA) using FastStart Universal Probe Master (Roche). Universal ProbeLibrary (UPL) probes were labeled with fluorescein (FAM) at the 5′ end and a dark quencher dye at the 3′ end. UPL probes contain 8-mer motif and annealed within PCR amplicon amplified by specific primers. The fluorophore was released by degradation of UPL probe during extension with DNA polymerase. Accumulation of PCR products was detected by monitoring the increased fluorescent signal. The primers as well as the UPL probes were designed with the UPL assay design center (www.universal-

probelibrary.com). The 5′ and 3′ mouse ACSL1 gene-specific primers and probe sequence were 5′-AAA GAT GGC TGG TTA CAC ACG-3′ (sense) and 5′-CGA TAA TCT TCA AGG TGC CAT T-3′ (antisense); UPL probe number 46 (5′-ATGGCTGC-3′); the 5′ and 3′ mouse ACSL3 gene-specific primers and probe sequence were 5′-TGC ACA GGC GTG TTT TAT GT-3′ (sense) and 5′-TGG ACC TCC CAG AGT AGC AT-3′ (antisense); UPL probe number 11 (5′-GCTGGAAG-3′); the 5′ and 3′ mouse ACSL5 gene-specific primers and probe sequence were 5′-ACC CAT GAA AAT GTT GTT TCA A-3′ (sense) and 5′-GAG GTG GGC TGG AAG ATA GG-3′ (antisense); UPL probe number 46 (5′-ATGGCTGC-3′); the 5′ and 3′ mouse GRP78 gene-specific primers and probe sequence were 5′-ATC GGA CGC ACT TGG AAT-3′ (sense) and 5′-CGG TTT AGT TTT CTT TTC AAC CA-3′ (antisense); UPL probe number 18 (5′-CAGCAGGA-3′); the 5′ and 3′ mouse β-actin gene-specific primers and probe sequence were 5′-ACT GCT CTG GCT CCT AGC AC-3′ (sense) and 5′-CTG GAA GGT GGA CAG TGA GG-3′ (antisense); UPL probe number 58 (5′-GGATGGAG-3′); the 5′ and 3′ human ACSL3 gene-specific primers and probe sequence were 5′-CAA GGG CAT CAT TGT GCA T-3′ (sense) and 5′-GGG CAA TGG TTT GCT ATG AG-3′ (antisense); UPL probe number 46 (5′-ATGGCTGC-3′); the 5′ and 3′ human GAPDH gene-specific primers and probe sequence were 5′-AGC CAC ATC GCT CAG ACA C-3′ (sense) and 5′-GCC CAA TAC GAC CAA ATC C-3′ (antisense); UPL probe number 60 (5′-TGGGGAAG-3′); the 5′ and 3′ human GSK-3β gene-specific primers and probe sequence were 5′-CAA ATT AAG GCA CAT CCT TGG-3′ (sense) and 5′-GTT AGT CGG GCA GTT GGT GT-3′ (antisense); UPL probe number 67 (5′-CTCCAGCA-3′). The cycling conditions were 50°C for 2 min and 95°C for 10 min, followed by 42 cycles of 95°C for 15 sec and 60°C for 1 min. The quantitative reverse transcription-PCR data were analyzed by the ΔΔCt method. All primers and probes were tested and the amplification efficiency were above 0.9 (0.95–1.01). The fluorescence signal intensities were quantified as a Ct (threshold cycle) value with the Sequence Detection System (SDS) Software 2.2 (Applied Biosystems). Gene expression levels were calibrated using human GAPDH or mouse β-actin expression levels as an internal control. Subtraction of the Ct value for a gene of interest from the Ct value for GAPDH yielded the ΔCt values. The ΔCt was normalized to the ΔCt of the control group to obtain the ΔΔCt values. The $2^{\Delta\Delta Ct}$ values of the treated groups were compared to the control groups and presented as fold changes as compared to the control condition.

### OIL RED O STAINING

After treatment, the cells were washed with cold PBS (137 mM NaCl, 2.7 mM KCl, 10 mM $Na_2HPO_4$, and 1.8 mM $KH_2PO_4$) and fixed for 15 min with 7.5% formaldehyde. The stock solution of Oil red O (5 mg/ml) in isopropyl alcohol was diluted to 60% with Milli-Q water. The Oil red O solution was filtered through a 0.22-μm syringe filter and incubated with the cells for 15 min. After washing with Milli-Q water, stained triglyceride droplets were visualized and photographed by light microscopy. To quantify the Oil red O staining, the stained area was measured using computer-assisted image quantification (Image-Pro Plus Software; Media Cybernetics, Inc., Silver Spring, MD), and the percent of the total cell surface covered by lipid droplets was calculated.

### RNA INTERFERENCE

siRNAs targeting ACSL1 and ACSL3 were constructed within the pHsU6 vector as described previously [Lu et al., 2006]. The following target sequences were used: 5′-GGG CAG ATC CAA CTC AGA A-3′ (nucleotides 2904–2922 of ACSL1 from the start codon); 5′-GGT TAT TCT TGG ACA GTA T-3′ (nucleotides 829–847 of ACSL3 from the start codon); and 5′-CGT GTT TAT TCT GGC CTA TAA-3′ (nucleotides 1666–1684 of ACSL3 from the start codon). HuH-7 cells were cotransfected with the pHsU6 vectors containing the shRNA that targeted the appropriate sequences and with pcDNA3.1 (−) using the LipofectAMINE 2000 transfection reagent (Invitrogen). The stable transfectants were selected with G418. The expression levels of ACSL1 and ACSL3 in HuH-7 stable transfectants were analyzed by RT-PCR with specific primers.

### IN VIVO INDUCTION OF ER STRESS BY TUNICAMYCIN

C57BL/6 mice were administered tunicamycin (1.5 mg/kg body weight) intraperitoneally. The mice were sacrificed at the indicated times, and the livers were removed and cryosectioned (5 μm) for Oil red O staining. To confirm the induction of ER stress by tunicamycin, the livers were also sampled, and the expression of GRP78 was examined by RT-PCR.

### STATISTICAL ANALYSIS

All statistical analyses were performed using Student's paired *t*-test. Data were expressed as the mean, and error bars represented the standard error of the mean from three independent experiments.

## RESULTS

### ER STRESS-INDUCED LIPID ACCUMULATION WAS ATTENUATED BY TRIACSIN C

Human hepatocarcinoma HuH-7 cells and immortalized mouse liver ML-1 cells were treated with tunicamycin, an ER stress inducer, and the cell lipid content was examined with Oil red O staining. Tunicamycin upregulated the expression of GRP78 (Fig. 1A), a chaperone protein, and increased the total lipid content (Fig. 1B,C). We then investigated the effects of the inhibitors Triacsin C, PD98059 (ERK inhibitor), JNK inhibitor II and GSK-3β inhibitor VIII on lipid accumulation. Among these inhibitors, the GSK-3β inhibitor caused an approximately 50% decrease in lipid accumulation, whereas Triacsin C was the most potent one and almost completely attenuated lipid accumulation (Fig. 1D). Because the targets of Triacsin C are long-chain acyl-CoA synthetase (ACSL) 1, 3, and 4, the expression of the ACSL gene family was determined during tunicamycin treatment.

### LONG-CHAIN Acyl-CoA SYNTHETASES (ACSLS) ARE UPREGULATED BY ER STRESS

HuH-7 cells were treated with tunicamycin, and the protein expression levels of ACSL1, 3, 4, 5, and 6 were further analyzed by Western blotting. The protein expression level of ACSL3 was upregulated by tunicamycin in HuH-7 cells and HepG2 cells (Fig. 2A,B). The increase in ACSL3 protein expression was abolished by addition of the translation inhibitor cycloheximide (Fig. 2C). An

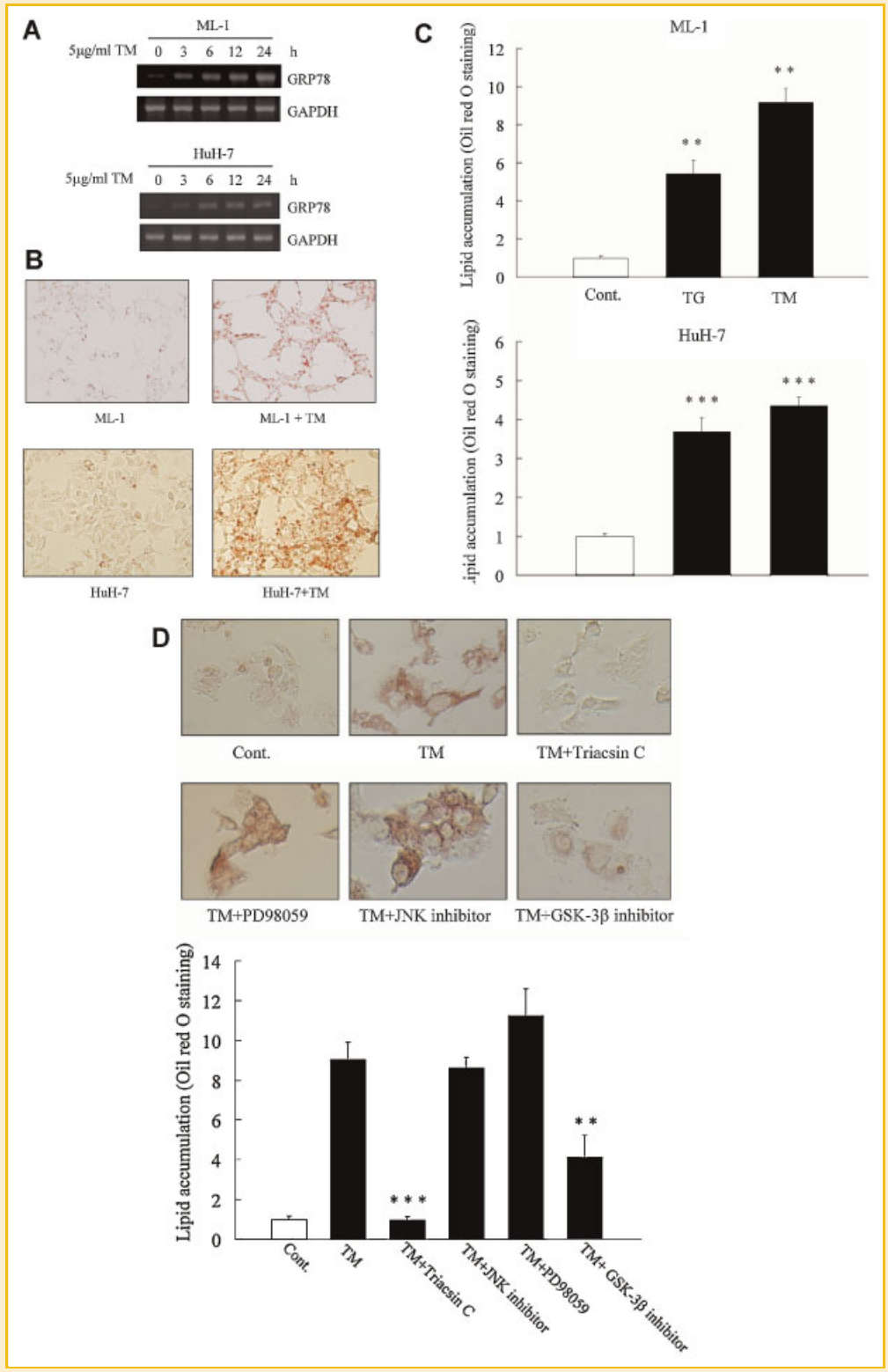


Fig. 1. Triacsin C inhibited ER stress-induced intracellular lipid droplets. A: ML-I and HuH-7 cells were treated with tunicamycin (TM) for 0, 3, 6, 12, or 24 h. Total RNA was isolated and then subjected to RT-PCR analysis. B: The accumulation of neutral lipids in ML-I (upper panel) and HuH-7 (lower panel) cells were visualized by Oil red O staining 24 h after tunicamycin treatment. C: Quantification of the Oil red O staining of ML-I (upper panel) and HuH-7 cells (lower panel) treated with thapsigargin (TG) and tunicamycin (TM). D: HuH-7 cells were co-treated with tunicamycin and the following inhibitors: 25 μM Triacsin C, 5 μM Erk inhibitor (PD98059), 5 μM JNK inhibitor II, or 20 μM GSK-3β inhibitor VIII for 24 h. The accumulation of neutral lipids in cells was visualized by Oil red O staining and quantified. $^{**}P < 0.01$ and $^{***}P < 0.001$ compared with the control group.

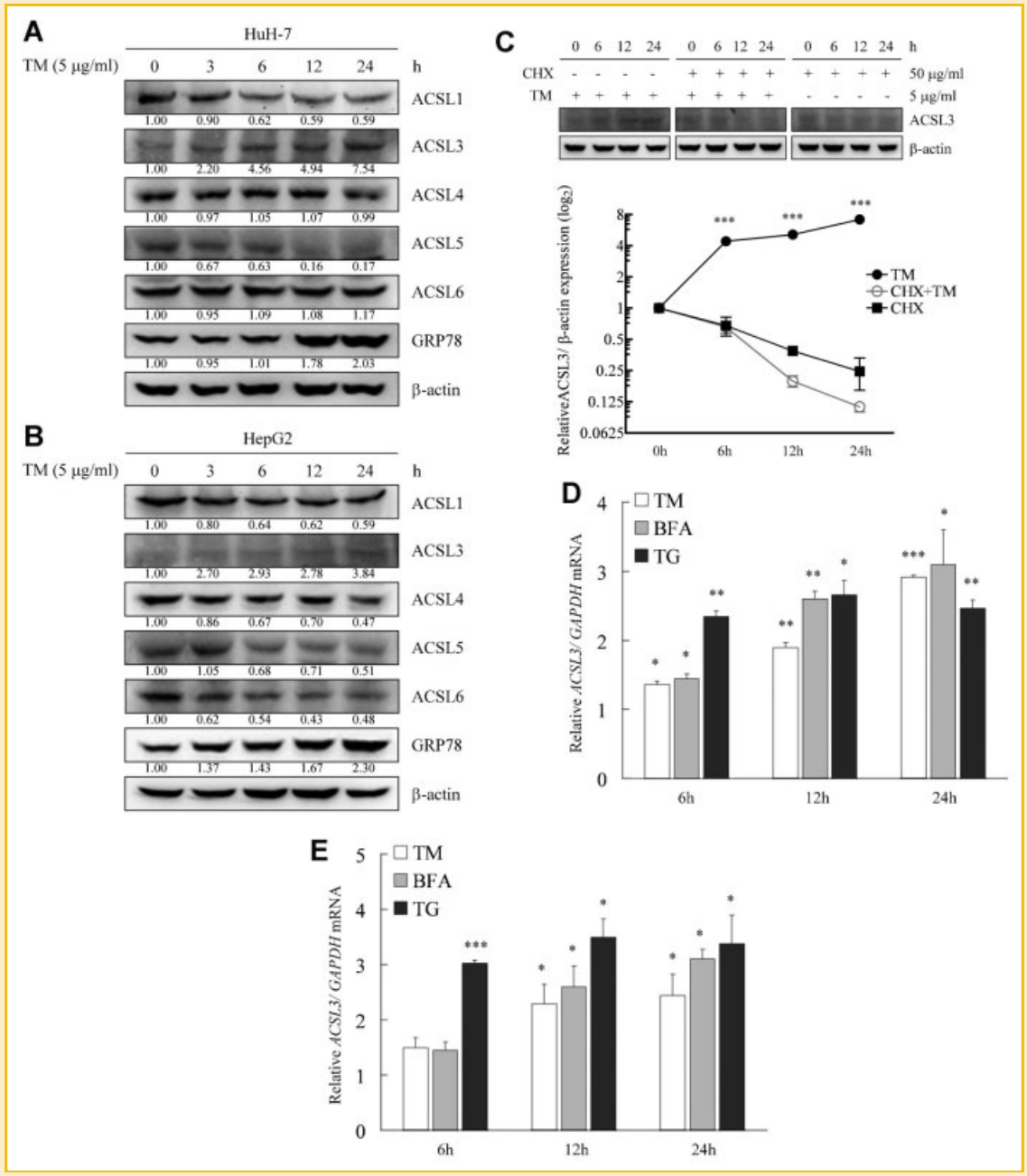


Fig. 2. Expression of ACSL3 is upregulated by ER stress. A: HuH-7 cells and (B) HepG2 cells were treated with TM for 0, 3, 6, 12, or 24 h, and the total cell lysate was isolated. The proteins in the cell lysates were subjected to Western blotting analysis using antibodies specific for ACSL1, ACSL3, ACSL4, ACSL5, ACSL6, GRP78, and β-actin. GRP78 was used as an indicator of ER stress, whereas β-actin was used as an internal control. C: HuH-7 cells were pretreated with cycloheximide (CHX) for 0.5 h before TM treatment, and the proteins in the cell lysates were subjected to Western blot analysis. $^{***}P < 0.005$ compared with the cycloheximide plus tunicamycin-treated group. D: HuH-7 cells and (E) HepG2 cells were treated with tunicamycin (TM), brefeldin A (BFA), and thapsigargin (TG) for 0, 3, 6, 12, or 24 h, and ACSL3 expression was determined by quantitative RT-PCR. GAPDH was used as an internal control. $^{*}P < 0.05$ and $^{**}P < 0.01$ compared with the control group.

increase in the mRNA expression of ACSL3 was also observed when HuH-7 cells were treated with other ER stress inducers, including brefeldin A (BFA) and thapsigargin (TG) (Fig. 2D). Similar inductions were observed in HepG2 cells (Fig. 2E). No significant changes of ACSL3 mRNA were observed in HuH-7 cells and HepG2 cells over 24 h without drug treatment (Fig. S2).

## ACSL3 IS INDUCED IN MOUSE LIVERS

We then determined the expression profiles of the ACSL family members and lipid accumulation in the livers of mice with ER stress. Mice were administered tunicamycin, and the expression of the ACSL family members in two mouse livers was analyzed. Lipid accumulation was observed in mouse livers after treatment with

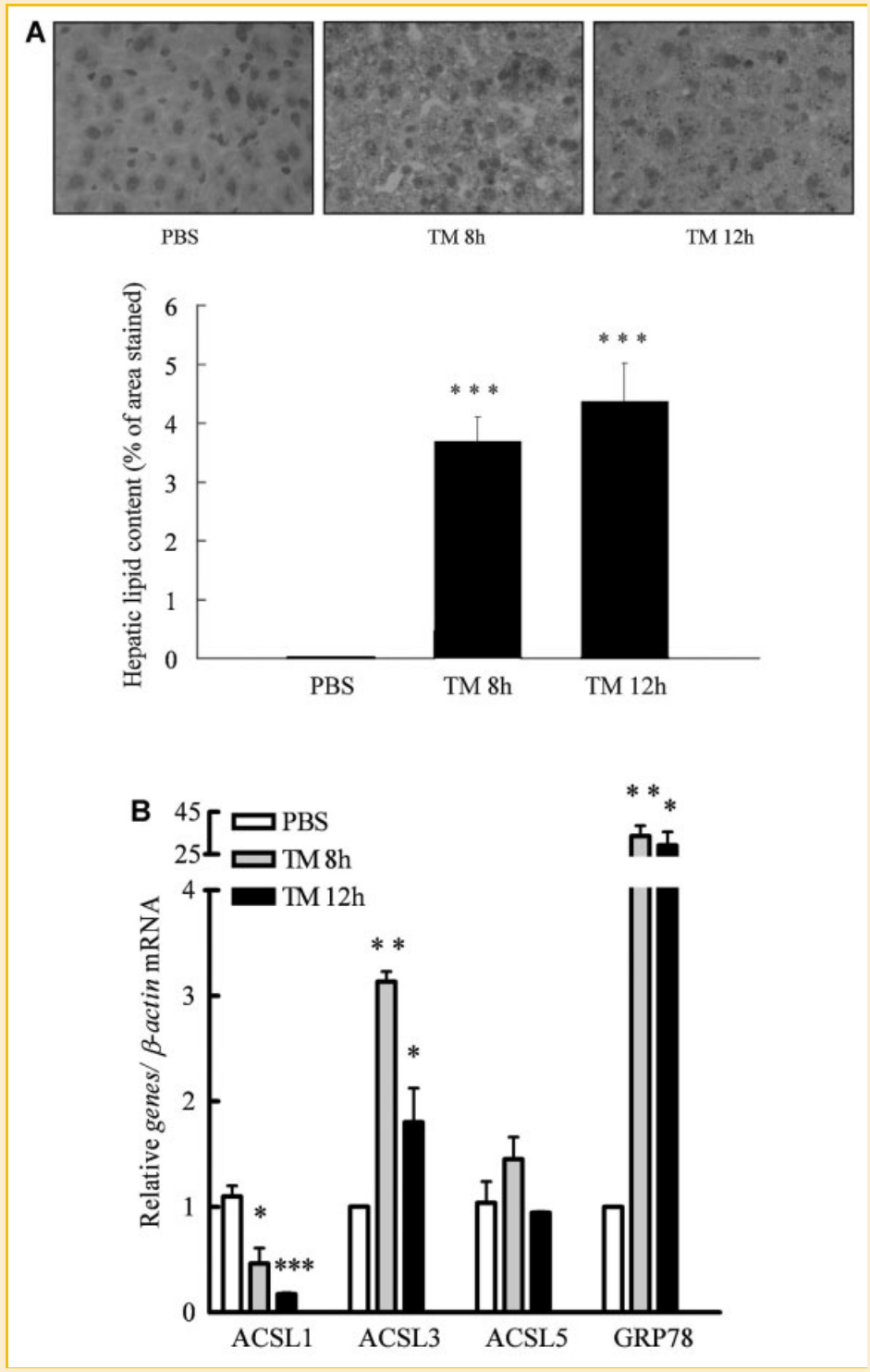


Fig. 3. Expression of ACSL3 is regulated by ER stress in vivo. C57BL/6 mice were intraperitoneally injected with tunicamycin (1.5 mg/kg) or a vehicle control (PBS). After 8 or 12 h, mice were sacrificed. A: Liver tissue was preserved with Tissue-Tek OCT. Sections of frozen livers were fixed in formaldehyde and stained with Oil red O. The quantification of the lipid content of two mice per group is shown. B: Liver tissue was homogenized in liquid nitrogen. Total RNA was isolated and then subjected to quantitative RT-PCR analysis using primers specific to ACSL1, ACSL3, ACSL5, GRP78, and β-actin. $^{*}P < 0.05$, $^{**}P < 0.01$, and $^{***}P < 0.001$ compared with the PBS group.

tunicamycin (Fig. 3A). Tunicamycin selectively induced the expression of ACSL3 and GRP78; in contrast, ACSL1 and 5 were decreased or unchanged (Fig. 3B).

### LONG-CHAIN Acyl-CoA SYNTHETASE 3 IS ESSENTIAL FOR LIPID ACCUMULATION INDUCED BY ENDOPLASMIC RETICULUM STRESS

Because expression of the ACSL3 gene was induced by ER stress, and because an inhibitor of ACSL1, 3, and 4 abolished lipid accumulation, we sought to determine whether ACSL3 was essential for lipid accumulation. HuH-7 cells were transfected with ACSL1 or ACSL3 siRNA, and stable clones were established. The ACSL-specific siRNAs efficiently downregulated the expression of the corresponding ACSLs, and these siRNAs did not have off-target effects on the expression of other ACSL family members was demonstrated by RT-PCR and western blotting (Fig. 4A,B and Fig. S1). Two independent stable transfectants were selected for each ACSL siRNA. The ACSL1 siRNA (shRNA 2904) did not affect ER-stress induced lipid accumulation (Fig. 4C); however, the ACSL3 siRNA (shRNA 829) inhibited the induction of lipid accumulation during ER stress (Fig. 4D). To exclude any off-target effects, we established two stable clones for another siRNA (shRNA 1666) that was directed against a different sequence of ACSL3 (Fig. 4E). The ACSL3 shRNA 1666 also effectively attenuated the induction of ACSL3 by ER stress (Fig. 4F). HuH-7 cells were also transfected with the ACSL5 shRNA and selected for stable transfectants. The ACSL5 shRNA did not affect lipid upregulation by ER stress (data not shown). These results indicated that ACSL3 was essential for lipid accumulation induced by ER stress.

### LINK BETWEEN ACSL3 AND GSK-3β

In addition to Triacsin C, we found that GSK-3β inhibitor VIII also attenuated lipid accumulation (Fig. 1D). We first determined whether GSK-3β was activated during ER stress. Tunicamycin activated GSK-3β as indicated by the decrease in Ser9 phosphorylation in HuH-7 cells (Fig. 5A). Therefore, we wanted to determine the relationship between ACSL3 and GSK-3β during the attenuation of lipid accumulation. Two GSK-3β inhibitors, LiCl and GSK-3β inhibitor VIII, attenuated the induction of ACSL3 by ER stress (Fig. 5B) and reduced lipid accumulation in HuH-7 cells (Fig. 5C). The roles of GSK-3β in lipid accumulation and ACSL-3 induction were further examined by depleting GSK-3β with a specific shRNA. HuH-7 and HepG2 cells were then transfected with GSK-3β shRNA, and stable transfectants were established (Fig. S3). Downregulation of GSK-3β inhibited the induction of ACSL3 (Fig. 5D,E) and lipid accumulation during ER stress (Fig. 5F). Based on the results of the GSK-3β inhibitors and shRNA, the inhibition of lipid accumulation by downregulating GSK-3β was correlated with the attenuation of ACSL3.

### Pre-S2 DELETION LARGE HEPATITIS B SURFACE PROTEIN (ΔS2-LHBs) INDUCED ER STRESS, ACSL3 EXPRESSION, AND LIPID ACCUMULATION

Our previous study demonstrated that the Pre-S2 deletion large hepatitis B surface protein induced ER stress, NF-κB activation, and COX-2 expression [Hung et al., 2004]. We investigated whether lipid induction and signal transduction was similarly regulated by the native ER stress inducer ΔS2-LHBs. The expression of the ACSL family and lipid content were examined in HuH-7 cells that express ΔS2-LHBs. The ACSL3 protein was selectively induced, while ACSL1 and 5 were downregulated (Fig. 6A). Similarly, Triacsin C effectively blocked lipid accumulation (Fig. 6B). Furthermore, GSK-3β inhibitors decreased the expression of ACSL3 and lipid accumulation (Fig. 6C,D). In conclusion, ACSL3 and GSK-3β inhibitors reduced ACSL3 expression and lipid accumulation in HuH-7 cells that express ΔS2-LHBs.

## DISCUSSION

In this report, we demonstrated that lipid content and long-chain acyl-CoA synthetase (ACSL) 3 were upregulated by ER stress in HuH-7 cells and mice livers. ACSL3 was required for lipid accumulation induced by ER stress in liver cells as demonstrated by the results from the ACSL3-targeted siRNA experiment. Finally, the induction of ACSL3 was in part mediated by GSK-3β. Inhibitors of ACSL3 or GSK-3β might be a useful therapy for lipid accumulation in the liver.

ACSL3 has been associated with the formation of lipid droplets in HuH-7 cells [Fujimoto et al., 2004]. Furthermore, the exogenous addition of oleic acid enhanced lipid droplet formation, which was accompanied by the increased expression of ACSL3 [Fujimoto et al., 2007]. In addition to neutral lipids, ACSL3 was essential for the formation of very low density lipoproteins (VLDL) in HuH-7 cells [Yao and Ye, 2008]. VLDL production is known to be involved in the secretion of hepatitis C virus particles from infected hepatocytes. Downregulation of ACSL3 by small interfering RNA decreased fatty acid synthesis by altering the activity of transcription factors, such as peroxisome proliferator activation receptor-γ and carbohydrate-responsive element-binding protein [Bu et al., 2009]. In this report, we further demonstrated that ER stress induced the upregulation of ACSL3, which was essential for lipid accumulation. Previous reports have suggested that ACSL1 plays an important role in liver lipid accumulation by examining the effects of ACSL1 overexpression [Li et al., 2006; Parkes et al., 2006]. A liver-specific knockout of ACSL1 decreased triacylglycerol levels and altered the fatty acid composition of phospholipids [Li et al., 2009]. In contrast, adenoviral-mediated overexpression of ACSL5 increased fatty acid uptake and triacylglycerol levels in rat hepatoma cells [Mashek et al., 2006]. The discrepancy between these reports is currently not well understood. However, the ACSL family members appear to play varying roles in hepatocytes through differential cellular localization and substrate preferences [Soupene and Kuypers, 2008]. The transcription factors that control lipid metabolism, such as sterol regulatory element-binding protein 1c (SREBP1c), are regulated by fatty acids or their metabolites [Xu et al., 2001]. The transcriptional activity of hepatocyte nuclear factor 4 was differentially regulated by long-chain fatty acyl-CoAs and depended on the level of unsaturation [Hertz et al., 1998]. Oleic acid increased glucose-6-phosphatase promoter activity, whereas polyunsaturated fatty acids suppressed the same promoter activity by modulating hepatocyte nuclear factor 4α [Rajas et al., 2002]. The pool of long-chain fatty acyl-CoA was differentially affected by alterations in ACSL gene expression and

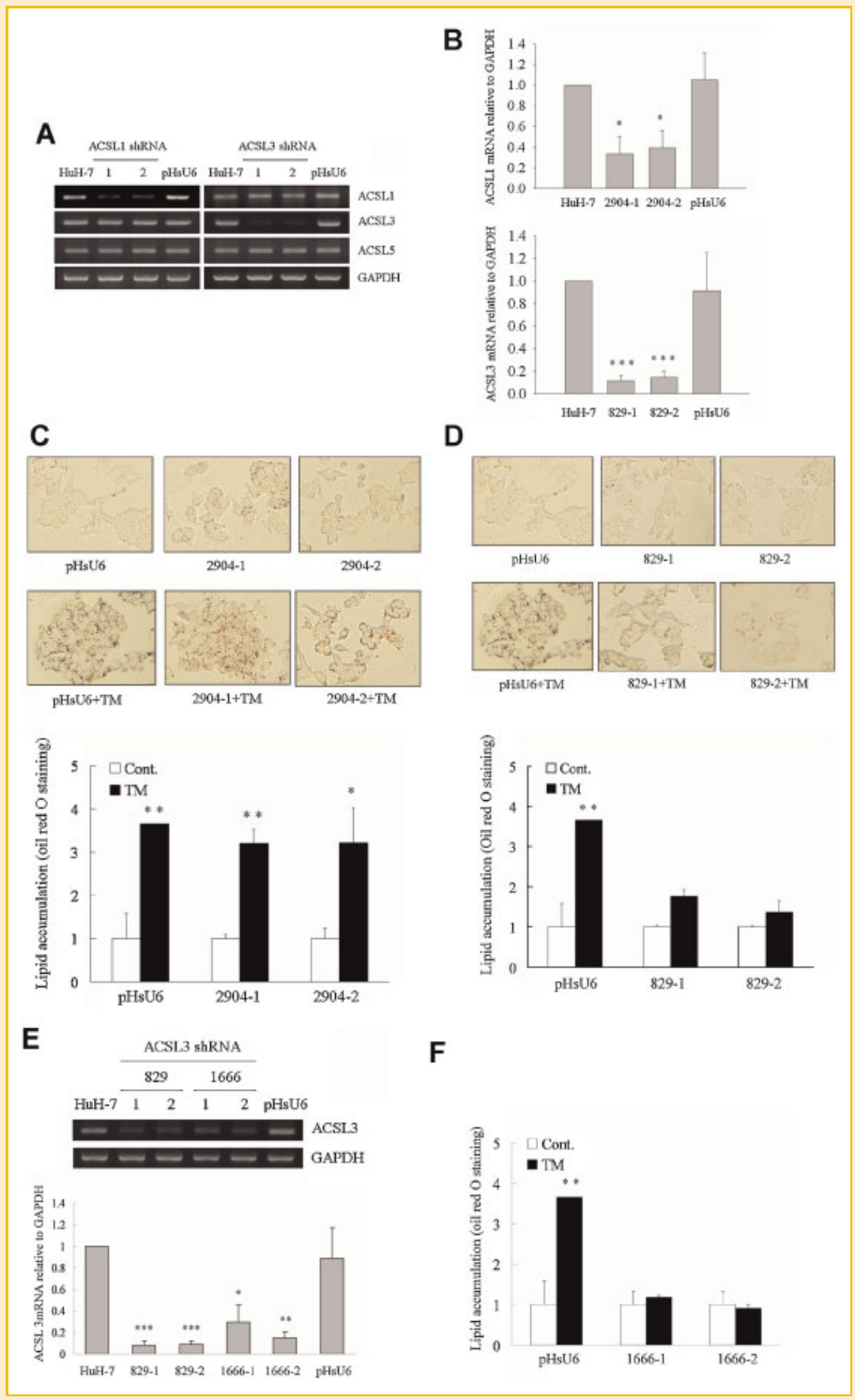


Fig. 4. ACSL3 shRNA inhibits lipid accumulation. A: The mRNA levels of ACSL family members in cells transfected with ACSL1 and ACSL3 shRNA or control cells. Total RNA was isolated and then subjected to RT-PCR analysis using primers specific for the ACSL family members and GAPDH. (B) Quantification of ACSL1 and ACSL3 expression in shRNA-transfected and control cells. $^{*}P < 0.05$ and $^{***}P < 0.001$ compared with the HuH-7 group. C: ACSL1 shRNA transfectants and (D) ACSL3 shRNA (ACSL3-829) transfectants were treated with 5 μg/ml tunicamycin for 24 h, and intracellular neutral lipids were visualized by Oil red O staining. The quantification of lipid content is shown in the lower panel. $^{*}P < 0.05$ and $^{**}P < 0.01$ compared with the control group. E: An ACSL3 shRNA (ACSL3-1666) that targets a different sequence also reduced ACSL3 expression. Two different stable clones were selected and assayed for the expression of ACSL3 during ER stress with RT-PCR. Quantification of ACSL3 expression by densitometry is shown in the lower panel. $^{*}P < 0.05$, $^{**}P < 0.01$, and $^{***}P < 0.001$ compared with the HuH-7 group. F: ACSL3 shRNA (ACSL3-1666) transfectants and control cells were treated with 5 μg/ml tunicamycin for 24 h, and the accumulation of lipids in cells was visualized by Oil red O staining and quantified. $^{**}P < 0.01$ compared with the control group.

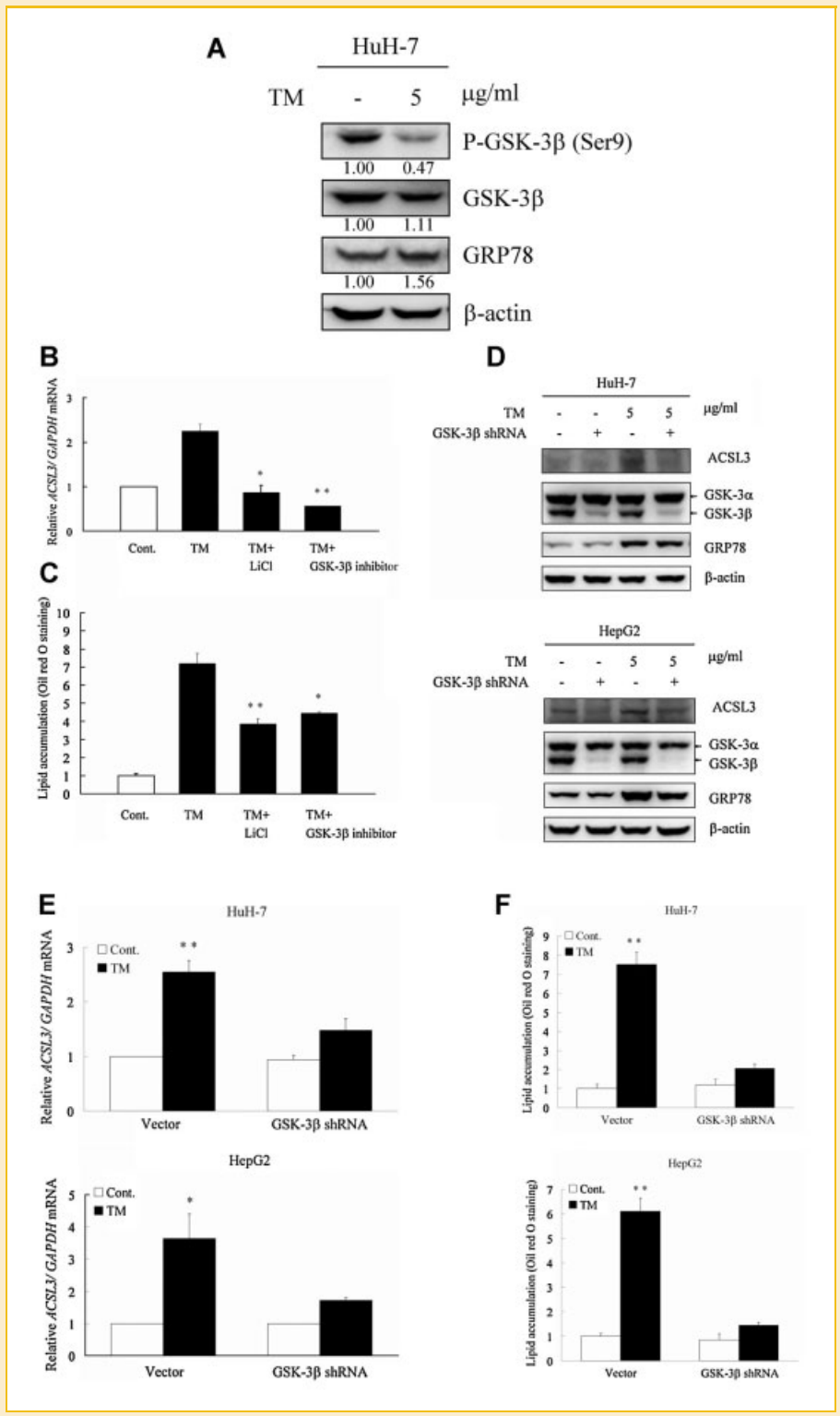


Fig. 5. GSK-3β is required for the induction of ACSL3 and lipid accumulation. A: HuH-7 cells were treated with 5 μg/ml tunicamycin for 24 h, and total protein was subjected to Western analysis using antibodies specific for P-GSK-3β, GSK-3β, GRP78, and β-actin. B: HuH-7 cells were treated with 5 μg/ml tunicamycin, and 40 mM LiCl or 20 μM GSK-3β inhibitor VIII for 24 h, and ACSL3 mRNA expression was determined with quantitative PCR. C: The lipid content in HuH-7 cells after incubation with 40 mM LiCl or 20 μM GSK-3β inhibitor VIII for 24 h. $^{*}P < 0.05$ and $^{**}P < 0.01$ compared with the TM group. D: HuH-7 (upper panel) and HepG2 cells (lower panel) vector control and GSK-3β shRNA transfectants were treated with tunicamycin (TM) for 24 h; the total protein was isolated and then subjected to western analysis using antibodies specific for ACSL3, GSK-3α/β, GRP78, and β-actin. E: ACSL3 mRNA expression levels in HuH-7 (upper panel) and HepG2 (lower panel) vector controls and GSK-3β RNAi transfectants were determined with quantitative PCR during TM treatment for 24 h. F: HuH-7 (upper panel) and HepG2 (lower panel) vector controls and GSK-3β shRNA transfectants were treated with 5 μg/ml tunicamycin for 24 h, and the accumulation of lipids in cells was visualized by Oil red O staining and quantified. $^{*}P < 0.05$ and $^{**}P < 0.01$ compared with the control group.

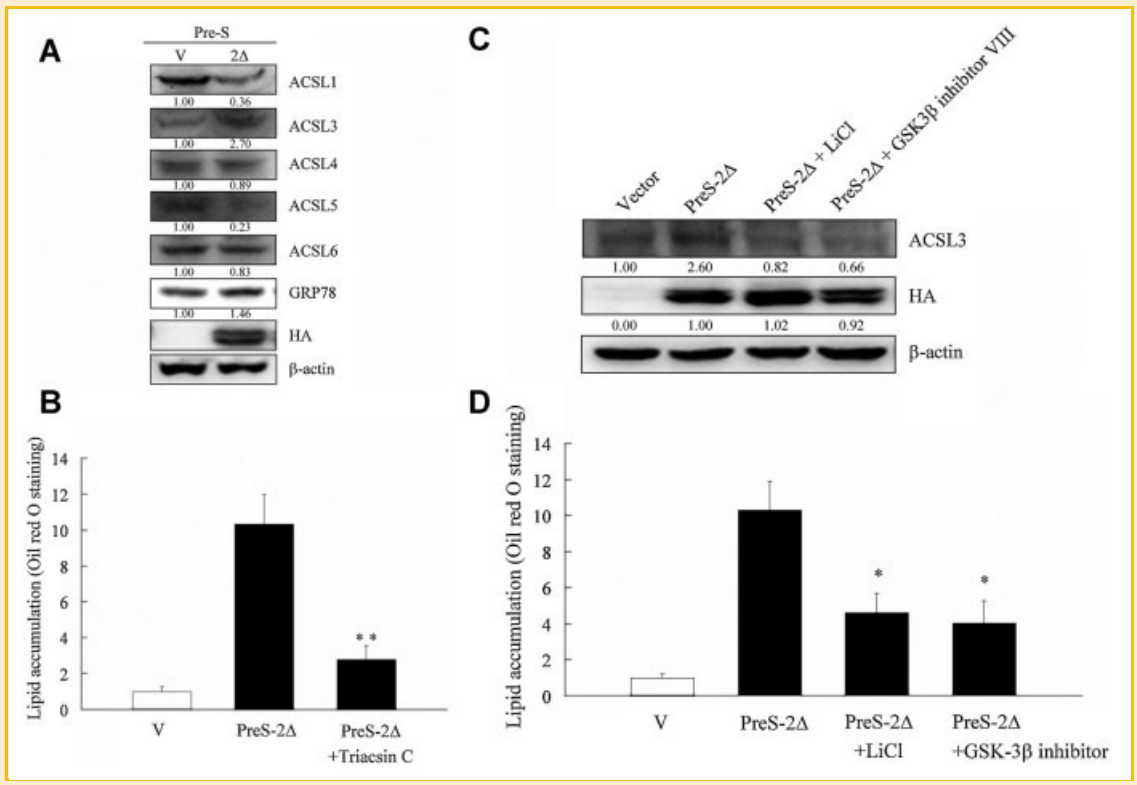


Fig. 6. GSK-3β and ACSL3 are required for lipid accumulation in HuH-7 cells that express the PreS2 deletion (PreS-2Δ) mutant HBV large surface protein. A: The expression of ACSL family members, HA-ΔS2-LHBs and GRP78 in ΔS2-LHBs transfectants or control cells was determined with Western blotting. B: PreS-2Δ transfectants were treated with 25 μM Triacsin C for 24 h, and the neutral lipids were visualized by Oil red O staining. C: PreS-2Δ transfectants were treated with 40 mM LiCl or 20 μM GSK-3β inhibitor VIII for 24 h, and the expression of the ACSL3 protein was determined by western blotting. D: The lipids of cells after the indicated treatments in PreS-2Δ transfectants were visualized with Oil red O staining and quantified. $^{*}P < 0.05$ and $^{**}P < 0.01$ compared with the PreS-2Δ transfectant group.

may be responsible for the differences in lipid contents. Our results and prior reports [Hertz et al., 1998; Xu et al., 2001; Rajas et al., 2002; Bu et al., 2009] suggested that altering the ACSL3 expression level, either by upregulating ER stress or by downregulating ACSL3 with shRNA, might change the pool of fatty acyl-CoAs, which leads to changes in transcription factor activity and causes lipid accumulation in the cell types examined here. However, we would not rule out the possibility that the activity of other ACSL family proteins may be altered during ER stress without affecting protein expression. In this fashion, ACSL3 shRNA or triacsin may also affect lipid upregulation by counteracting other ACSL family members.

The upstream sensors and signaling components that contribute to the endoplasmic reticulum stress response have been shown to be associated with abnormalities in lipid metabolism. ATF6 and NF-κB binding sites have been detected in the promoter of ACSL gene family members. Although both of these transcription factor binding sites are present in the promoters of the ACSL1, 3, and 4 genes, the regulation of ACSL genes is not solely determined by these two transcription factors because ACSL3 is the only member induced by ER stress. It is likely that other signaling pathways induced by ER stress may help to determine which ACSL genes are upregulated by ER stress. In this report, we demonstrated that GSK-3β regulated ACSL3 expression; GSK-3β has been shown to affect NF-κB and STAT family members in the inflammatory process [Steinbrecher et al., 2005; Beurel and Jope, 2008]. In addition, GSK-3β is also involved in the cytosolic localization of p53 during ER stress, which prevents p53-dependent apoptosis [Qu et al., 2004; Baltzis et al., 2007]. Downregulation of GSK-3β inhibits the NF-κB signaling pathway during the death of glioma cells and hepatocytes [Götschel et al., 2008; Kotliarova et al., 2008]. GSK-3β might activate ACSL3 through the activation of NF-κB; however, GSK-3β is involved in multiple pathways, such as the tumor necrosis factor-alpha converting enzyme downstream pathway [Fiorentino et al., 2010], and may regulate lipid droplet formation through other pathways in addition to ACSL3.

In summary, ER stress causes lipid accumulation by increasing the expression of ACSL3 and activating GSK-3β which is involved in the enhanced expression of ACSL3. These results may provide a new therapeutic approach for the dysregulation of lipid metabolism in the liver by ER stress.

## ACKNOWLEDGMENTS

This work was supported in part by grant number NSC 95-2311-B-006-001 to Dr. Ming-Derg Lai from the National Science Council, Taiwan, Republic of China, by Innovative and Exploratory Project grant number B035 from National Cheng Kung University, and by

grant DOH99-TD-C-111-03 to the Comprehensive Cancer Center in Southern Taiwan.

## REFERENCES


Baltzis D, Pluquet O, Papadakis AI, Kazemi S, Qu LK, Koromilas AE. 2007. The eIF2alpha kinases PERK and PKR activate glycogen synthase kinase 3 to promote the proteasomal degradation of p53. J Biol Chem 282:31675–31687.

Beurel E, Jope RS. 2008. Differential regulation of STAT family members by glycogen synthase kinase-3. J Biol Chem 283:21934–21944.

Bu SY, Mashek MT, Mashek DG. 2009. Suppression of long chain acyl-CoA synthetase 3 decreases hepatic de novo fatty acid synthesis through decreased transcriptional activity. J Biol Chem 284:30474–30483.

Coleman RA, Lewin TM, Muoio DM. 2000. Physiological and nutritional regulation of enzymes of triacylglycerol synthesis. Annu Rev Nutr 20:77–103.

Fiorentino L, Vivanti A, Cavalera M, Marzano V, Ronci M, Fabrizi M, Menini S, Pugliese G, Menghini R, Khokha R, Lauro R, Urbani A, Federici M. 2010. Increased tumor necrosis factor alpha-converting enzyme activity induces insulin resistance and hepatosteatosis in mice. Hepatology 51:103–110.

Fujimoto Y, Itabe H, Sakai J, Makita M, Noda J, Mori M, Higashi Y, Kojima S, Takano T. 2004. Identification of major proteins in the lipid droplet-enriched fraction isolated from the human hepatocyte cell line HuH7. Biochim Biophys Acta 1644:47–59.

Fujimoto Y, Itabe H, Kinoshita T, Homma KJ, Onoduka J, Mori M, Yamaguchi S, Makita M, Higashi Y, Yamashita A, Takano T. 2007. Involvement of ACSL in local synthesis of neutral lipids in cytoplasmic lipid droplets in human hepatocyte HuH7. J Lipid Res 48:1280–1292.

Gaspar ML, Jesch SA, Viswanatha R, Antosh AL, Brown WJ, Kohlwein SD, Henry SA. 2008. A block in ER-to-golgi trafficking inhibits phospholipid synthesis and induces neutral lipid accumulation. J Biol Chem 283:25735–25751.

Goodman JM. 2008. The gregarious lipid droplet. J Biol Chem 283:28005–28009.

Götschel F, Kern C, Lang S, Sparna T, Markmann C, Schwager J, McNelly S, von Weizsäcker F, Laufer S, Hecht A, Merfort I. 2008. Inhibition of GSK3 differentially modulates NF-kappaB, CREB, AP-1 and beta-catenin signaling in hepatocytes, but fails to promote TNF-alpha-induced apoptosis. Exp Cell Res 314:1351–1366.

Harding HP, Novoa I, Zhang Y, Zeng H, Wek R, Schapira M, Ron D. 2000. Regulated translation initiation controls stress-induced gene expression in mammalian cells. Mol Cell 6:1099–1108.

Hertz R, Magenheim J, Berman I, Bar-Tana J. 1998. Fatty acyl-CoA thioesters are ligands of hepatic nuclear factor-4alpha. Nature 392:512–516.

Hsu IR, Kim SP, Kabir M, Bergman RN. 2007. Metabolic syndrome, hyperinsulinemia, and cancer. Am J Clin Nutr 86:s867–s871.

Hu P, Han Z, Couvillon AD, Kaufman RJ, Exton JH. 2006. Autocrine tumor necrosis factor alpha links endoplasmic reticulum stress to the membrane death receptor pathway through IRE1alpha-mediated NF-kappaB activation and down-regulation of TRAF2 expression. Mol Cell Biol 26:3071–3084.

Huang WC, Lin YS, Chen CL, Wang CY, Chiu WH, Lin CF. 2009. Glycogen synthase kinase-3beta mediates endoplasmic reticulum stress-induced lysosomal apoptosis in leukemia. J Pharmacol Exp Ther 329:524–531.

Hung JH, Su IJ, Lei HY, Wang HC, Lin WC, Chang WT, Huang W, Chang WC, Chang YS, Chen CC, Lai MD. 2004. Endoplasmic reticulum stress stimulates the expression of cyclooxygenase-2 through activation of NF-kappaB and pp38 mitogen-activated protein kinase. J Biol Chem 279:46384–46392.

Jiang HY, Wek SA, McGrath BC, Scheuner D, Kaufman RJ, Cavener DR, Wek RC. 2003. Phosphorylation of the alpha subunit of eukaryotic initiation factor 2 is required for activation of NF-kappaB in response to diverse cellular stresses. Mol Cell Biol 23:5651–5663.

Kang H, Lee SK, Kim MH, Choi H, Lee SH, Kwack K. 2009. Acyl-CoA synthetase long-chain family member 6 is associated with premature ovarian failure. Fertil Steril 91:1339–1343.

Kotliarova S, Pastorino S, Kovell LC, Kotliarov Y, Song H, Zhang W, Bailey R, Maric D, Zenklusen JC, Lee J, Fine HA. 2008. Glycogen synthase kinase-3 inhibition induces glioma cell death through c-MYC, nuclear factor-kappaB, and glucose regulation. Cancer Res 68:6643–6651.

Lee AH, Scapa EF, Cohen DE, Glimcher LH. 2008. Regulation of hepatic lipogenesis by the transcription factor XBP1. Science 320:1492–1496.

Lewin TM, Kim JH, Granger DA, Vance JE, Coleman RA. 2001. Acyl-CoA synthetase isoforms 1, 4, and 5 are present in different subcellular membranes in rat liver and can be inhibited independently. J Biol Chem 276:24674–24679.

Li LO, Mashek DG, An J, Doughman SD, Newgard CB, Coleman RA. 2006. Overexpression of rat long chain acyl-coa synthetase 1 alters fatty acid metabolism in rat primary hepatocytes. J Biol Chem 281:37246–37255.

Li LO, Ellis JM, Paich HA, Wang S, Gong N, Altshuller G, Thresher RJ, Koves TR, Watkins SM, Muoio DM, Cline GW, Shulman GI, Coleman RA. 2009. Liver-specific loss of long chain acyl-CoA synthetase-1 decreases triacylglycerol synthesis and beta-oxidation and alters phospholipid fatty acid composition. J Biol Chem 284:27816–27826.

Lu TJ, Lai WY, Huang CY, Hsieh WJ, Yu JS, Hsieh YJ, Chang WT, Leu TH, Chang WC, Chuang WJ, Tang MJ, Chen TY, Lu TL, Lai MD. 2006. Inhibition of cell migration by autophosphorylated mammalian sterile 20-like kinase 3 (MST3) involves paxillin and protein-tyrosine phosphatase-PEST. J Biol Chem 281:38405–38417.

Mashek DG, McKenzie MA, Van Horn CG, Coleman RA. 2006. Rat long chain acyl-CoA synthetase 5 increases fatty acid uptake and partitioning to cellular triacylglycerol in McArdle-RH7777 cells. J Biol Chem 281:945–950.

Matsuda D, Namatame I, Ohshiro T, Ishibashi S, Omura S, Tomoda H. 2008. Anti-atherosclerotic activity of triacsin C, an acyl-CoA synthetase inhibitor. J Antibiot (Tokyo) 61:318–321.

Obata Y, Fukumoto Y, Nakayama Y, Kuga T, Dohmae N, Yamaguchi N. 2010. The Lyn kinase C-lobe mediates Golgi export of Lyn through conformation-dependent ACSL3 association. J Cell Sci 123:2649–2662.

Oyadomari S, Harding HP, Zhang Y, Oyadomari M, Ron D. 2008. Dephosphorylation of translation initiation factor 2alpha enhances glucose tolerance and attenuates hepatosteatosis in mice. Cell Metab 7:520–532.

Pahl HL, Baeuerle PA. 1996. Activation of NF-kappa B by ER stress requires both Ca2+ and reactive oxygen intermediates as messengers. FEBS Lett 392:129–136.

Parkes HA, Preston E, Wilks D, Ballesteros M, Carpenter L, Wood L, Kraegen EW, Furler SM, Cooney GJ. 2006. Overexpression of acyl-CoA synthetase-1 increases lipid deposition in hepatic (HepG2) cells and rodent liver in vivo. Am J Physiol Endocrinol Metab 291:E737–E744.

Pluquet O, Qu LK, Baltzis D, Koromilas AE. 2005. Endoplasmic reticulum stress accelerates p53 degradation by the cooperative actions of Hdm2 and glycogen synthase kinase 3beta. Mol Cell Biol 25:9392–9405.

Qu L, Huang S, Baltzis D, Rivas-Estilla AM, Pluquet O, Hatzoglou M, Koumenis C, Taya Y, Yoshimura A, Koromilas AE. 2004. Endoplasmic reticulum stress induces p53 cytoplasmic localization and prevents p53-dependent apoptosis by a pathway involving glycogen synthase kinase-3beta. Genes Dev 18:261–277.

Rajas F, Gautier A, Bady I, Montano S, Mithieux G. 2002. Polyunsaturated fatty acyl coenzyme A suppress the glucose-6-phosphatase promoter activity by modulating the DNA binding of hepatocyte nuclear factor 4 alpha. J Biol Chem 277:15736–15744.

Raven JF, Baltzis D, Wang S, Mounir Z, Papadakis AI, Gao HQ, Koromilas AE. 2008. PKR and PKR-like endoplasmic reticulum kinase induce the proteasome-dependent degradation of cyclin D1 via a mechanism requiring eukaryotic initiation factor 2alpha phosphorylation. J Biol Chem 283:3097–3108.

Reddy JK, Rao MS. 2006. Lipid metabolism and liver inflammation. II. Fatty liver disease and fatty acid oxidation. Am J Physiol Gastrointest Liver Physiol 290:G852–G858.

Rutkowski DT, Wu J, Back SH, Callaghan MU, Ferris SP, Iqbal J, Clark R, Miao H, Hassler JR, Fornek J, Katze MG, Hussain MM, Song B, Swathirajan J, Wang J, Yau GD, Kaufman RJ. 2008. UPR pathways combine to prevent hepatic steatosis caused by ER stress-mediated suppression of transcriptional master regulators. Dev Cell 15:829–840.

Soupene E, Kuypers FA. 2008. Mammalian long-chain acyl-CoA synthetases. Exp Biol Med (Maywood) 233:507–521.

Starley BQ, Calcagno CJ, Harrison SA. 2010. Nonalcoholic fatty liver disease and hepatocellular carcinoma: A weighty connection. Hepatology 51:1820–1832.

Steinbrecher KA, Wilson W III, Cogswell PC, Baldwin AS. 2005. Glycogen synthase kinase 3beta functions to specify gene-specific, NF-kappaB-dependent transcription. Mol Cell Biol 25:8444–8455.

Thiele C, Spandl J. 2008. Cell biology of lipid droplets. Curr Opin Cell Biol 20:378–385.

Wang HC, Chang WT, Chang WW, Wu HC, Huang W, Lei HY, Lai MD, Fausto N, Su IJ. 2005. Hepatitis B virus pre-S2 mutant upregulates cyclin A expression and induces nodular proliferation of hepatocytes. Hepatology 41:761–770.

Wang D, Wei Y, Pagliassotti MJ. 2006. Saturated fatty acids promote endoplasmic reticulum stress and liver injury in rats with hepatic steatosis. Endocrinology 147:943–951.

Xu J, Teran-Garcia M, Park JH, Nakamura MT, Clarke SD. 2001. Polyunsaturated fatty acids suppress hepatic sterol regulatory element-binding protein-1 expression by accelerating transcript decay. J Biol Chem 276:9800–9807.

Yang JC, Teng CF, Wu HC, Tsai HW, Chuang HC, Tsai TF, Hsu YH, Huang W, Wu LW, Su IJ. 2009. Enhanced expression of vascular endothelial growth factor-A in ground glass hepatocytes and its implication in hepatitis B virus hepatocarcinogenesis. Hepatology 49:1962–1971.

Yao H, Ye J. 2008. Long chain acyl-CoA synthetase 3-mediated phosphatidylcholine synthesis is required for assembly of very low density lipoproteins in human hepatoma Huh7 cells. J Biol Chem 283:849–854.

Ye J, Rawson RB, Komuro R, Chen X, Dave UP, Prywes R, Brown MS, Goldstein JL. 2000. ER stress induces cleavage of membrane-bound ATF6 by the same proteases that process SREBPs. Mol Cell 6:1355–1364.